

## OPTIMIZATION AND *IN VITRO* EVALUATION OF LAPATINIB-ENCAPSULATED LIPOMER SUSPENSION FOR EFFECTIVE CANCER THERAPY

NIGAR KADAR MUJAWAR<sup>1</sup>, JAMEEL AHMED S. MULLA<sup>2\*</sup>

<sup>1</sup>Shree Santkrupa College of Pharmacy, Ghogaon, Karad-415111, Maharashtra, India. <sup>2\*</sup>Department of Pharmaceutics, Shree Santkrupa College of Pharmacy, Ghogaon, Karad-415111, Maharashtra, India

\*Corresponding author: Jameel Ahmed S. Mulla; \*Email: [jameelahmed5@gmail.com](mailto:jameelahmed5@gmail.com)

Received: 15 Oct 2025, Revised and Accepted: 02 Feb 2026

### ABSTRACT

**Objective:** To establish and optimize a lipomer-based formulation of lapatinib (LAP) for addressing issues of poor solubility, bioavailability, drug release and stability.

**Methods:** Lipomer were synthesized using emulsification and solvent evaporation (ESE) methods. Optimization was performed for three critical formulation parameters: PLA, Soya lecithin, and DCM using a 3<sup>3</sup> central composite design (CCD) with a quality by design (QbD) approach. Characterization techniques included FTIR, DSC, FESEM, and TEM to evaluate structural integrity and drug entrapment. In vitro drug release studies and three-month stability studies at 4±2 °C and 40±2 °C, 75% relative humidity (RH) were conducted.

**Results:** Optimized formulation had the following physicochemical properties: particle size (PS): 88.5 nm, zeta potential (ZP): -22.2 mV, polydispersity index (PDI): 0.194, entrapment efficiency (%EE): 85.15%, cumulative drug release (%CDR): 88.85%, FTIR, DSC, FESEM, and TEM confirmed preserved structure and successful drug entrapment. In vitro release showed sustained, continuous drug release and stability studies indicated that the formulation remained stable under the tested conditions.

**Conclusion:** The lipomer-based delivery system enhances the solubility, bioavailability, and stability of LAP, offering a promising strategy for sustained drug delivery.

**Keywords:** Lapatinib, Lipomer, Drug delivery system, Quality by design, Central composite design, Stability study

© 2026 The Authors. Published by Innovare Academic Sciences Pvt Ltd. This is an open access article under the CC BY license (<https://creativecommons.org/licenses/by/4.0/>) DOI: <https://dx.doi.org/10.22159/ijap.2026v18i2.57180> Journal homepage: <https://innovareacademics.in/journals/index.php/ijap>

### INTRODUCTION

Lung cancer is one of the leading causes of cancer death worldwide, with non-small cell lung cancer (NSCLC) accounting for nearly 85% of the cases identified. The vast majority of cases of NSCLC have poor prognoses despite major improvements in early screening and management; this is attributed to its high aggressiveness, nonconformity to treatment, and high rate of spreading to other parts of the body [1]. Although so common, conventional chemotherapy has been restricted by a lack of specificity, gross systemic toxicity, and poor healing effects. Therefore, a significant demand exists to find more potent and focused treatment approaches that deliver more positive patient outcomes with fewer side effects [2, 3]. LAP is a potent dual tyrosine kinase inhibitor of Epidermal Growth Factor Receptor (EGFR/ErbB1) and Human Epidermal Growth Factor Receptor 2 (HER2/ErbB2) that blocks their phosphorylation and downstream pathways such as PI3K-Akt and MAPK, thus inhibiting tumour growth and survival. It is clinically effective in HER2-positive breast cancer and is considered for lung tumours with EGFR/HER2 overexpression. However, in NSCLC, its utility is limited by low and variable oral bioavailability, largely owing to very poor aqueous solubility and marked dependence on gastric pH and food intake for absorption. High plasma protein binding ( $\approx$  99%) and rapid hepatic metabolism (especially via CYP3A4) further reduce drug levels at the tumour, increasing off-target exposure and toxicity risk. Thus, improved delivery systems through lipid polymer hybrid nanoparticle (Lipomer/IPHNPs) will play a vital role in this [4-6].

Lipomer, a new type of nanocarrier in the form of hybrids between liposomes and polymeric nanoparticles, with structural and functional characteristics of both, has become a promising alternative. They are generally a polymeric core (e. g., polylactic acid (PLA)) and lipid core (e. g., soya lecithin) and have the features of longer times, enhanced stability, high drug-loading capacity, and also being biocompatible. Lipomer have the capability of offering a better dose protection to the drug, effective trapping of hydrophobic drugs such as LAP, as well as sustained

release behaviour, thus regardless of the pharmacokinetics and pharmacodynamics of the donor drug dispersed within the particle [6, 7].

The aim and goal of this research is to design and optimize a LAP-encapsulated lipomer suspension for effective therapy. Enhance solubility, bioavailability and drug release. Use a QbD-based 3<sup>3</sup> CCD approach to formulate and optimize lipomer. Characterize the formulation, evaluate in vitro release, and assess its therapeutic potential.

### MATERIALS AND METHODS

#### Chemicals and reagent

LAP was obtained from Distinct Lifecare Mumbai. Sigma-Aldrich (Mumbai, India) provided soya lecithin. All other chemicals used in the formulation, like PLA, dichloromethane (DCM), acetic acid, stearylamine and polyvinyl alcohol (PVA) were sourced from Unique Biological and Chemicals, Kolhapur, Maharashtra, India. The dialysis membranes procured from the Sigma Aldrich product in Darmstadt, Germany, had dialysis molecular weight cut-offs ranging from 12,000 to 14,000. The other solvents and chemicals are mainly of analytical grade and purified. This selection of materials ensures high quality and consistency for the development of LAP-loaded lipomer suspension.

#### Instrument/Equipment used

The study utilised various laboratory instruments, including a UV-visible spectrophotometer (Shimadzu model 1800, Japan). FTIR (Bruker Alpha II ATR), Electronic balance (Digital Mettler Toledo MS105 MS Semi Micro Balances), DSC TGA (USA SDT 600), XRD (Bruker AXS D8 Advance), Probe Sonicator (pks 500F), Centrifuge (Remi RM-12 centrifuge), Freeze Dryer (Martin Christ, Alpha 2-4 ISC), Zetasizer and Particle Size Analyser (Horbia Nanopartica SZ 100), FESEM (FEI, Quanta 200F), SEM (JEOL JSM IT-200) TEM (JEOL, JEM-2100 and Plus, Japan) and Stability Chamber (Remi Electrotechnique Lim. Vasai).

### Preparation of LAP lipomer suspension

In this method, the organic phase consisted of PLA 30 mg, soya-lecithin 46.41 mg, and stearylamine 9 mg dissolved in 7.99 ml DCM, along with LAP (200 mg) dissolved in 0.3 ml acetic acid. The mixing was achieved using an ESE method. The organic phase was introduced dropwise into the 20 ml of 1.5% w/v PVA aqueous solution under high-speed mechanical stirring for 24 h (table 1). Because DCM is immiscible with water, the slow addition of the organic phase allowed it to disperse into fine organic droplets within the continuous aqueous phase stabilized by PVA. High-speed stirring imparted enough shear to break the organic phase into small, uniform droplets, preventing phase separation and minimizing the formation of a coarse water-in-oil emulsion. During 24 h of continued stirring, the DCM gradually evaporated, causing the organic droplets to harden into lipomer, while PVA stabilized their surface and prevented aggregation. The resulting nanoparticle dispersion was probe-sonicated at 4 °C in 5-minute cycles with 3-minute rests to prevent thermal degradation. Lipomer has been obtained by centrifuging at 10,000 rpm for a period of 20 min at 4 °C, rinsing 3 times using distilled water, reconstituted in Millipore water, and subsequently kept in an airtight container for further analysis [8-10].

### Formulation optimization by DOE

Optimizing LAP-loaded lipomer suspension using the DoE approach, as well as the effect of factors on the selection of the optimal formulation. To develop the batches that met our objectives, we used Design-Expert® version 13. This program evaluates all replies simultaneously. A 3<sup>2</sup>-CCD was used to study the effect of particular factors on the formulation of an LAP-loaded lipomer suspension. The program provided 20 formulations, including eight factorial points, six axial points, and six duplicated centers. The CCD design matrix is shown in table 2.

To evaluate three process variables, PLA (X<sub>1</sub>), soya lecithin(X<sub>2</sub>), and DCM (X<sub>3</sub>), LAP lipomer suspension formulations were optimized using CCD (table 1). The aim was to assess formulation sensitivity at

low (-1) (0) and high (+1) levels. Three-factor, three-level Central CCD was used. Five dependent variables included PS (Y<sub>1</sub>), ZP (Y<sub>2</sub>), PDI (Y<sub>3</sub>), %EE (Y<sub>4</sub>), and %CDR (Y<sub>5</sub>). Optimization targeted PS, PDI, %EE, and %CDR, while maintaining ZP within an optimal range. CCD enabled the evaluation of primary, quadratic, and interaction effects of independent variables, leading to predictive models. The desirability method was applied to optimize lipomer, enhancing relationships among response variables. Independent factors X<sub>1</sub> (10–30 mg), X<sub>2</sub> (4–70 mg), and X<sub>3</sub> (1–8 mg) were studied using CCD. Dependent responses included PS (minimized), ZP (in range), PDI (minimized), %EE (maximized), and %CDR (maximized). Each response was assigned desirability functions (0 = undesirable, 1 = most desired), with targets based on minimization or maximization. The overall desirability score was the geometric mean of individual values, and the formulation that received the highest scores was selected as optimum. Model validation used checkpoint analysis with random formulations, comparing predicted and experimental results. Prediction errors >5% required model refinement. This approach ensured accurate optimization with desirable physicochemical properties and improved drug release. Diagnostic plots and response surface methodology were used for validation. This DoE strategy successfully developed a stable formulation with optimized PS, stability, and drug release, ensuring maximum therapeutic efficacy [11-13].

### Response surface analysis (RSA)

The Design Expert was utilized for experimental design, with batches generated from 3<sup>2</sup> CCD. It is useful for ensuring that the design fits. We used analysis of variance (ANOVA), F tests, and correlation coefficients at a 95% significance level (p<0.05) for validating the data. The program contrasts the data and proposes batches based on our suggestions. We require batches with minimum PS, PDI, within ranges of ZP and % maximize %EE and %CDR to fill each requirement of sustained drug delivery, in relation to the recommendation that the batch be manufactured and further analyzed to validate the projected response [13].

**Table 1: Screened independent variables with their values**

Factors (independent variables)	Levels		
	Low (-1)	Medium (0)	High (+1)
Concentrations of PLA (X <sub>1</sub> ) mg	10	20	30
Concentrations of Soya-lecithin (X <sub>2</sub> ) mg	4	37	70
Concentrations of DCM (X <sub>3</sub> ) ml	1	4.5	8

### Characterization of lipomer suspension

#### Particle size, polydispersity index and zeta potential

LAP-loaded lipomer suspension in which PS and ZP were measured using dynamic light scattering (DLS) and a ZP analyzer. Samples were diluted in deionised water to prevent multiple scattering, placed in a cuvette, and analyzed at ambient temperature mean particle diameter, PDI, and size distribution assessed formulation homogeneity. Electrophoretic mobility determined ZP, reflecting surface charge density and colloidal stability. ZP values indicated electrostatic interactions, critical for preventing particle aggregation and ensuring dispersion stability.

#### Entrapment efficiency percentage (%EE)

The indirect method was employed in determining the %EE of LAP in the LAP-loaded lipomer suspension. 1 ml of dispersion was transferred into a centrifugation tube to separate the un-entrapped drug by centrifugation (Remi RM-12 microcentrifuge) at 15000rpm for 30 min. Then 10µl clear supernatant liquid was collected and diluted with methanol up to 10 ml, estimated at 357 nm, using a UV visible spectrophotometer [14]. By using the formula, the % EE [14].

$$EE\% = \left( \frac{\text{Amount of drug in Lipomer}}{\text{Total amount of drug added}} \right) \times 100$$

#### In Vitro drug release study of LAP-loaded lipomer suspension

The study assessed LAP permeation using dialysis membranes with a selected bi-chambered Franz diffusion cell apparatus (Electrolab

Diffusion Cell apparatus EDC-07). Drug concentration in the receptor compartment was measured at fixed intervals, while temperature and pH were monitored to mimic physiological conditions. The donor compartment was filled with the drug solution, and receptor samples were collected at 1-24 h via a sampling port (5 ml each) and replaced with 5 ml of phosphate buffer (pH 6.8), maintained at 37±0.5 °C with continuous stirring at 100 rpm and analyzed using UV-Vis spectroscopy. Data were used to calculate permeability coefficients, providing insight into drug absorption and bioavailability. This information is essential for optimizing the formulation and understanding structural changes that may affect absorption rates [13].

#### Fourier-transform infrared spectroscopy (FTIR)

To study the possible interactions of LAP with excipients within the LAP-loaded lipomer suspension, FTIR spectroscopy was also carried out. All the samples, namely, LAP and LAP-loaded lipomer suspension, were degassed by combining with potassium bromide (KBr) and pelleted into a disc form. Data were collected at a wavelength of 4000-400 cm fast-1 and characteristic peak frequencies were evaluated to show the functional groups present and chemical activities between [15].

#### Field emission scanning electron microscopy (FESEM)

Surface morphology of the LAP-loaded lipomer suspension was analysed employing FESEM. A tiny bit of lyophilised sample was put on a carbon-coated grid, vacuumed with a thinnest layer of gold over it with a sputter coater. They were taken under an electron beam at

various magnifications to discern the shape, the nature of the surface and the distribution of the particles [16].

### Transmission electron microscopy (TEM)

TEM investigation was performed to better investigate the underlying structure and shape of the LAP-loaded lipomer suspension. After being dyed with phosphotungstic acid and allowed to dry, a drop of the object being studied was placed onto a copper grid. The grid was then viewed in a TEM and recorded images captured using the transmission electron microscope at low, medium and high magnification to determine the particle shape, core-shell structure, and homogeneity of dispersion of the particles [17].

### Accelerated stability study

It was determined whether the LAP-loaded lipomer suspension remained stable over a three-month program at refrigerator temperature ( $4 \pm 2$  °C) and accelerated ( $40 \pm 2$  °C/75% RH) temperatures. This formulation was maintained in the amber coloured and corked glass vials, and each sample was drawn at 0, 1, 2, and 3 mo intervals to determine the PS, PDI, ZP %EE, and %CDR.

The formulation's stability was also calculated according to acceptable variations in PS, PDI, ZP, and % CDR is  $\pm 10\%$  and for %EE, not less than 90% of the initial, and used, and they were observed to be intact in both sets of storage conditions [10, 18].

## RESULTS AND DISCUSSION

### Formulation optimization by DOE

CCD was used to assess the influence of three factors,  $X_1$ ,  $X_2$ , and  $X_3$ , on LAP-loaded lipomer suspension optimization (table 2). The independent variables were examined at three levels and coded as (-1, 0,+1) while keeping all other formulation variables constant to assess their influence on  $Y_1$ ,  $Y_2$ ,  $Y_3$ ,  $Y_4$ , and  $Y_5$ . Optimization aimed to minimize PS and PDI, maintain ZP in the ideal range, and maximize %EE and %CDR. ANOVA, lack-of-fit, and correlation coefficient analyses were used to determine model significance and identify key influential factors. CCD enabled evaluation of main, quadratic, and interaction effects, generating predictive models. Diagnostic plots and response surface methodology verified model equations for optimal formulation. This DoE approach produced a stable, effective formulation [19, 20].

Table 2: CCD matrix with variables and observed response values

Formulation code	Factor 1 $X_1$	Factor 2 $X_2$	Factor 3 $X_3$	( $Y_1$ ) PS	( $Y_2$ ) ZP	( $Y_3$ ) PDI	( $Y_4$ ) %EE	( $Y_5$ ) %CDR
F1	0	0	-1	51.7	-18.1	0.281	88.94	95.39
F2	0	0	0	66.3	-23.1	0.369	82.31	86.65
F3	-1	0	0	66.3	-22.5	0.369	89.77	93.45
F4	-1	1	-1	66.3	-22.5	0.369	89.54	93.45
F5	-1	-1	-1	27.8	-23.9	1.8	89.79	92.48
F6	-1	1	1	129.1	-24.4	0.389	86.41	92.48
F7	0	0	0	130.2	-1.3	0.749	85.83	92.48
F8	1	0	0	66.3	-22.5	0.369	89.64	93.45
F9	1	1	-1	67.7	-14.6	0.357	91.75	96.84
F10	0	0	0	66.1	-16.5	0.821	89.66	91.5
F11	0	0	0	28.8	4	1.35	86.87	94.42
F12	1	-1	0	81.2	-23.7	0.461	89.78	97.82
F13	-1	-1	1	118.2	-14.1	0.525	89.51	97.82
F14	0	-1	1	116.7	-18.4	0.657	88.22	95.87
F15	1	1	1	118.2	-1.3	0.654	87.98	96.84
F16	1	0	1	66.3	-22.5	0.369	89.66	93.45
F17	0	1	0	98.2	-27.8	0.89	97.67	95.84
F18	0	0	0	66.3	-22.5	0.369	89.44	93.48
F19	0	0	0	187	-87	1	65.28	86.17
F20	0	-1	-1	87	-22	0.54	89.63	92.48

\*Mean $\pm$ SD (n=3), Factor 1  $X_1$ : Concentration of PLA (mg), Factor 2  $X_2$ : Concentration of soya-lecithin (mg), Factor 3  $X_3$ : Concentration of DCM (mg), ( $Y_1$ ) PS: Particle size, ( $Y_2$ ) ZP: Zeta Potential ( $Y_3$ ) PDI: Polydispersity Index ( $Y_4$ ) %EE: Entrapment Efficiency Percentage, %CDR: Cumulative drug release ( $Y_5$ ) [13].

Afterwards, the assessment software generates equations; the equation that comes out describes the interaction of independent variables. The resulting counterplots and surface response plots depict a diagrammatic link within the stated variables in table 2. Fig. 3 shows that changes in  $X_1$ ,  $X_2$ , and  $X_3$  have a significant impact on PS, ZP, PDI, % EE, and %CDR.

### Model analysis of PS

The PS of LAP-loaded lipomer suspension, ranging from 27.8 nm (F5) to 187 nm (F19), is strongly influenced by formulation parameters, affecting drug release, bioavailability, and therapeutic efficacy. The wide variation in particle size at the center points indicates that the lipomer formulation is highly sensitive to minor fluctuations in PLA, soya lecithin, and DCM levels. Center points normally show good reproducibility, but the large deviations suggest strong non-linear and interactive effects that influence droplet formation and particle solidification. The interactive model further confirmed significant impacts on ZP, PDI, %EE, and %CDR, demonstrating that the system does not behave uniformly near the midpoint of the design space. This highlights intrinsic formulation instability and represents a key limitation of using CCD for such

sensitive colloidal systems. PS and distribution are crucial in lipid core, controlling intracellular trafficking and biodistribution, with submicron particles offering advantages over microparticles. PLA, soya-lecithin, and DCM concentrations, along with their interactions, significantly impact PS. Two-factor interactions are key in predicting PS, and models using actual and coded factors can estimate responses for specific ingredient levels, guiding formulation design to enhance stability and therapeutic performance. PS of the suggested batch shown in fig. 1.

ZP is a key parameter influencing colloidal stability, with higher values preventing particle aggregation; the normal range is -30 to +30 mV. ZP ranges from -87 mV to +4 mV. An interactive factor model assessed the effects of  $X_1$ ,  $X_2$ , and  $X_3$  on ZP, showing significant interactions. Optimizing these components enhances stability and therapeutic efficacy while balancing drug encapsulation efficiency. Exploring other surfactants and concentrations may further improve stability. Stability studies under varying conditions are essential to ensure long-term preservation of therapeutic benefits, increasing formulation reliability and supporting future drug delivery system development. Fig. 1 B showing ZP of the suggested batch.

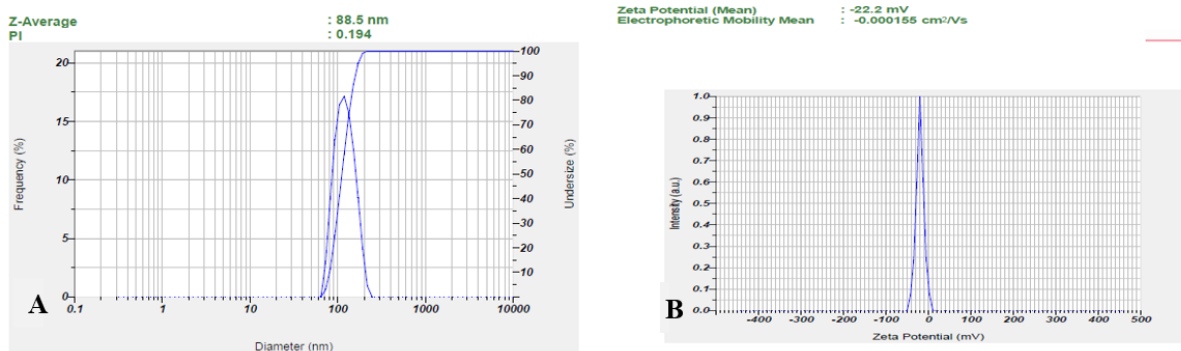


Fig. 1: A) Particle size distribution, B) Zeta potential of LAP-loaded lipomer suspension model analysis of ZP

**Model analysis of PDI**

PDI values closer to 0 indicate a more monodisperse system, while higher values (>0.5) indicate significant polydispersity. It reflects polymer molecular weight dispersion; low PDI shows a narrow distribution, high PDI indicates a broad distribution, affecting polymer performance. PDI is influenced by X<sub>1</sub>, X<sub>2</sub>, and X<sub>3</sub>, with significant interaction effects. The wide ZP range (-87 to +4 mV) occurred because PLA, lecithin, and DCM had strong non-linear interaction effects, revealed by CCD. High lecithin and low PLA created an extremely negative ZP (-87 mV). High PLA and low lecithin caused near-neutral ZP (+4 mV). CCD intentionally tests extremes, so large variations are expected. This helps determine the most stable formulation conditions. Optimizing these can yield uniform particles and enhance LAP drug delivery. Higher X<sub>1</sub> reduces particle size distribution, improving release, while higher X<sub>3</sub> broadens PDI. Surfactant choice, temperature, and excipient interactions also affect stability, bioavailability, and therapeutic outcomes [13, 21].

**Model analysis of %EE**

The % EE of LAP lipomer ranged from 97.85% (Formulation 15) to 64% (Formulation 19), influenced by X<sub>1</sub>, X<sub>2</sub>, and X<sub>3</sub> concentrations. Higher PLA enhances %EE via polymer matrix stability, though excessive amounts may reduce loading. Soya-lecithin modulates interfacial properties and release kinetics, while DCM affects polymer cross-linking and mechanical characteristics. Solvent type also impacts drug solubility, matrix stability, and encapsulation

effectiveness. Optimizing these factors is crucial to achieving high %EE and improved LAP-loaded lipomer suspension performance [13, 23-27].

**Model analysis of %CDR**

The CDR of LAP-loaded lipomer suspension ranged from 97.82% (Formulations 12 and 13) to 86.17% (Formulation 19), representing the percentage of drug released over time. %CDR of the suggested of batch shown in fig.2.%CDR is influenced by drug properties, polymer matrix, environment, molecular weight, additives, dosage design, surface area, and %EE. X<sub>1</sub>, X<sub>2</sub>, and X<sub>3</sub> significantly affect release, with higher concentrations accelerating CDR. PLA enhances diffusion, soya-lecithin modulates solubility and permeability, and DCM affects kinetics. Interaction effects require careful optimization to balance stability, sustained release, and bioavailability for improved therapeutic outcomes. The LAP-loaded lipomer suspension of the suggested batch exhibited sustained release, with 36% released in 2 h, 59.95% at 6 h, and 88.85% at 11 h. This slower release is attributed to LAP encapsulation within the polymeric matrix of nanoparticles. The cumulative percentage of drug release from nanoparticles showed initially burst release and sustained release thereafter. The sustained release is attributed to the presence of a lipid bilayer made up of lipid and stearylamine that acts as a rate-limiting membrane for the release of the encapsulated drug. The sustained release profile of LAP-loaded lipomer supports prolonged therapeutic levels, improved bioavailability, and highlights its use as a sustained medication delivery system. Triplicate measurements (mean±SD, n=3) confirmed reproducibility [10].

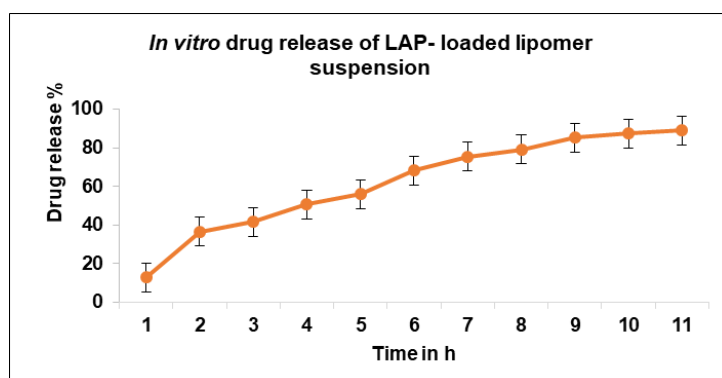


Fig. 2: In vitro drug release profile of LAP-loaded lipomer suspension [13]

Table 3: Polynomial equations in terms of coded factors

Parameters	Equation in terms of coded factors
PS	Y1 (PS) = +56.06 + 12.04 X <sub>1</sub> - 10.89 X <sub>2</sub> - 4.66 X <sub>3</sub> + 13.99 X <sub>1</sub> X <sub>2</sub> - 20.34 X <sub>1</sub> X <sub>3</sub> - 5.36 X <sub>2</sub> X <sub>3</sub> + 2.51 X <sub>1</sub> <sup>2</sup> + 9.86 X <sub>2</sub> <sup>2</sup> + 25.58 X <sub>3</sub> <sup>2</sup>
ZP	Y2 (ZP) = 178.98 + 3.90 X <sub>1</sub> - 41.55 X <sub>2</sub> - 12.06 X <sub>3</sub> - 16.00 X <sub>1</sub> X <sub>2</sub> - 51.75 X <sub>1</sub> X <sub>3</sub> - 6.25 X <sub>2</sub> X <sub>3</sub> + 178.98 X <sub>1</sub> <sup>2</sup> + 3.90 X <sub>2</sub> <sup>2</sup> - 41.55 X <sub>3</sub> <sup>2</sup>
PDI	Y3 (PDI) = +33.43 + 47.93X <sub>1</sub> +48.03X <sub>2</sub> +47.86X <sub>3</sub> +82.12X <sub>1</sub> X <sub>2</sub> +82.35 X <sub>1</sub> X <sub>3</sub> +82.13X <sub>2</sub> X <sub>3</sub>
%EE	Y4 (%EE) = +87.90 + 0.4933 X <sub>1</sub> +0.5681 X <sub>2</sub> +4.21 X <sub>3</sub>
%CDR	Y5 (%CDR) = +93.53 + 1.42 X <sub>1</sub> +0.0903X <sub>2</sub> +1.25X <sub>3</sub>

**Response surface analysis (RSA)**

RSA was used to optimize the LAP-loaded lipomer suspension by examining the effects of  $X_1$ ,  $X_2$ , and  $X_3$  on critical parameters. The optimized formulation achieved a maximum desirability of 0.905, targeting nanoparticle size, low PDI, maximum %EE, %CDR, and ZP within the desired range. mean values and a 95% prediction interval indicated high stability, potency, and reliability. Significant correlations among dependent variables suggested that improving one parameter could enhance others. Per cent prediction errors were under 5%, demonstrating the precision and robustness of the optimization. PS, ZP, PDI, %EE, and %CDR constants from five center point tests differed significantly ( $P < 0.05$ ), highlighting the need for iterative model refinement. Smaller PS correlated with slower dissolution and reduced bioavailability, while higher absolute ZP improved colloidal stability. Responses Y1–Y5 were converted into individual desirability scores (d1–d5) with equal weight; the optimal solution ( $D=1.00$ ) was PLA = 30 mg, soya-lecithin = 46.41 mg, and DCM = 7.99 ml. Point predictions showed mean PS ~92.76, narrow PDI, stable ZP, high %EE, and efficient %CDR. Observed and predicted responses closely matched, validating the model and

confirming the effectiveness of selected concentrations for reliable, therapeutically relevant drug delivery.

The predicted and actual values for the lapatinib-loaded lipomer suspension showed close agreement, validating the model's accuracy. The actual PS (88.5 nm) was slightly higher than predicted (81.97 nm), and the ZP (-22.2 mV) closely matched (-21.24 mV), indicating a stable and well-dispersed lipomer. A notably lower PDI (0.194) suggested a more uniform particle distribution, while the %EE (85.15%) was marginally below the predicted (87.90%), reflecting efficient drug encapsulation. The %CDR exhibited a minor deviation (88.85% vs. 93.53%), confirming sustained and controlled release behaviour consistent with the optimized formulation model. Predicted values for PS, PDI, ZP, %EE, and %CDR of the optimized formulation, as well as the actual values acquired following checkpoint analysis. The actual and predicted outcomes for every improved formulation are almost identical. This will reduce the amount of bias while offering a great correlation among variables. The modest bias verifies the derived model's validity and accuracy. Fig. 3 depicts 2D and 3D response plots that illustrate the impacts of factors on A) PS, B) ZP, C) PDI, D)% EE, and E)%CDR [27, 28].

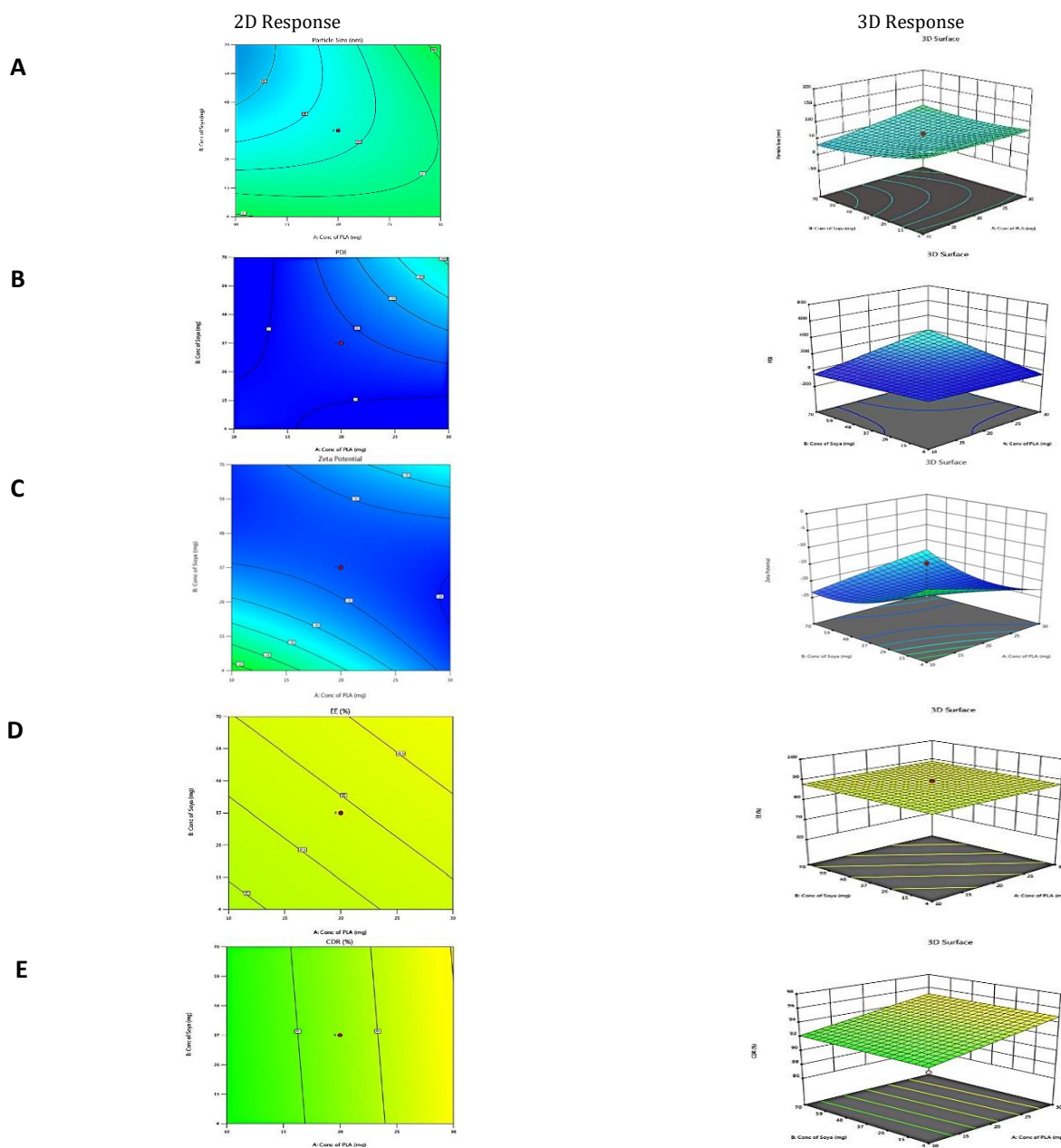


**Fig. 3: 2D and 3D response plots showing effects of variables on A) PS B) ZP C)PDI D)% EE E)%CDR**

### FTIR of LAP-loaded lipomer suspension

The FTIR spectrum of LAP (A) Physical mixture (B) and LAP-loaded lipomer suspension (C) fig. 4, showed characteristic peaks confirming the presence of the drug and excipients discussed as below

(A) Pure LAP: The FTIR spectrum of pure LAP shows sharp, distinct peaks corresponding to O-H/N-H stretching ( $3300\text{--}3500\text{ cm}^{-1}$ ), characteristic aromatic C=C stretching ( $\sim 1650\text{--}1500\text{ cm}^{-1}$ ), and C-O/C-N stretching ( $\sim 1100\text{ cm}^{-1}$ ). These sharp peaks confirm the intact functional groups and crystalline nature of LAP.

(B) Physical mixture: The physical mixture spectrum exhibits a simple superimposition of LAP, PLA, and soya lecithin peaks. The ester C=O band of PLA ( $\sim 1750\text{ cm}^{-1}$ ) and lipid  $\text{CH}_2$  stretching ( $2920/2850\text{ cm}^{-1}$ ) appear alongside all characteristic LAP peaks without any shifts. This indicates no interaction between the drug and excipients, confirming a mere physical blend.

(C) LAP-loaded lipomer suspension: A broad peak at  $3638\text{ cm}^{-1}$  indicated O-H stretching (hydrogen bonding). Peaks at  $2923$  and  $2748\text{ cm}^{-1}$  corresponded to C-H stretching. The sharp peak at  $1747\text{ cm}^{-1}$  indicated C=O stretching. Peaks at  $\sim 1637$  and  $\sim 1492\text{ cm}^{-1}$  reflected amide and C-H bending, while  $\sim 1310\text{--}1003\text{ cm}^{-1}$  indicated C-N and C-O stretching. Bands at  $811$  and  $676\text{ cm}^{-1}$  confirmed aromatic vibrations, indicating successful LAP incorporation without structural changes. So Marked reduction or broadening of LAP's characteristic peaks, Minor shifts in C=O and O-H/N-H regions, Dominance of PLA and lecithin peaks, and Absence of new functional group bands.

These changes indicate successful encapsulation of LAP within the lipomer matrix, accompanied by non-covalent interactions (primarily hydrogen bonding) between LAP and PLA/lecithin. The disappearance/weakened appearance of drug peaks confirms that LAP is molecularly dispersed and trapped inside the lipomer, rather than present as free crystalline drug.

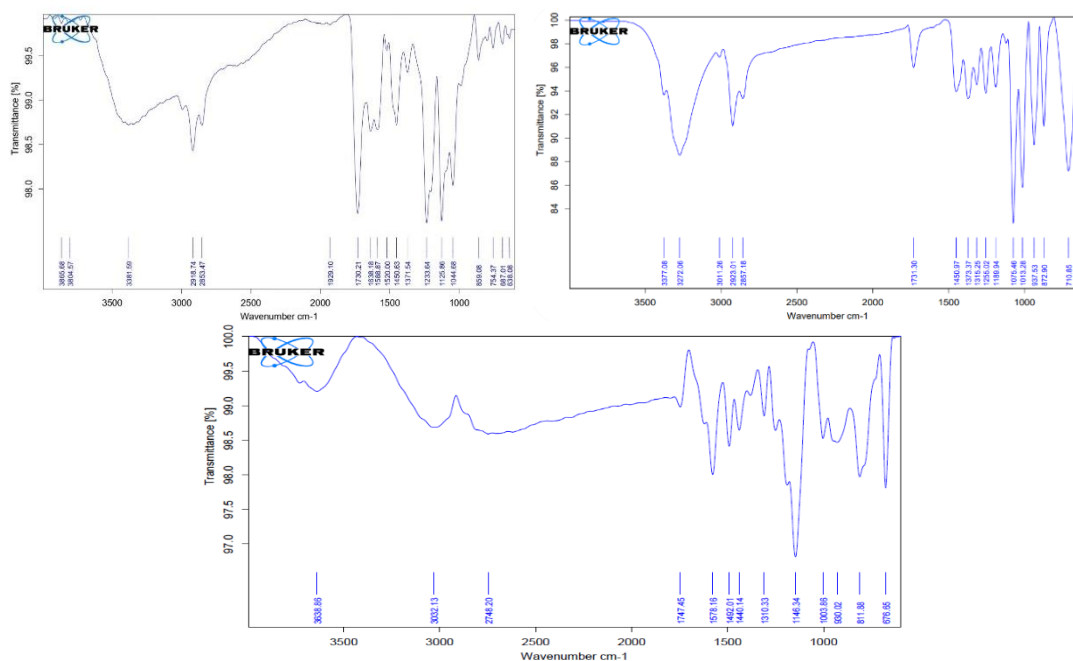


Fig. 4: FTIR of LAP (A) Physical mixture (B) and LAP-loaded lipomer suspension (C)

### FESEM of LAP-loaded lipomer suspension

An LAP lipomer suspension FESEM tomography fig. 5 at different magnifications revealed a relatively smooth surface morphology with uniformly dispersed nanoscale particles. The absence of large aggregates suggested good dispersion and stability of the lipomer formulation. The slightly visible fibrous structures in the FESEM images likely arise from partial PLA chain entanglement during

solvent evaporation, creating thin polymeric strands on the particle surface. Such structures can form when the polymer solidifies rapidly, trapping lecithin-rich domains and producing a faint fibrous network. This does not indicate instability but reflects the polymer-lipid interaction during lipomer formation. These fibrous features may also contribute to sustained drug release by reinforcing the structural integrity of the lipomer matrix. Overall, the morphology confirmed the successful formulation of a stable Lipomer system.

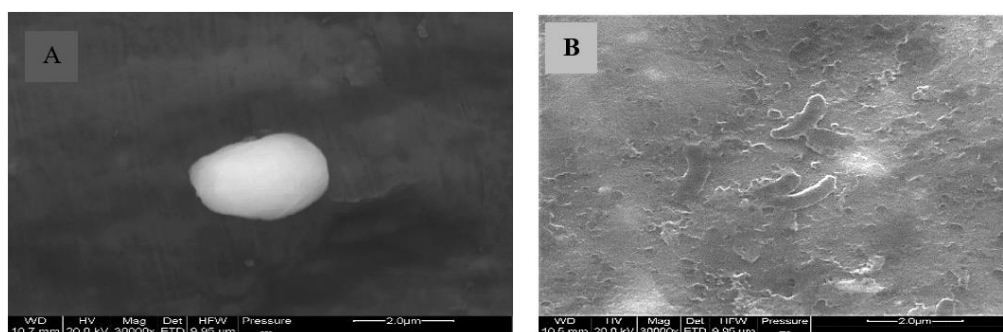


Fig. 5: A and B FESEM micrograph of LAP-loaded lipomer suspension

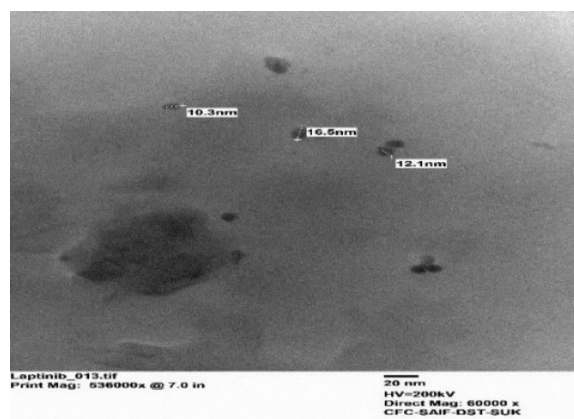


Fig. 6: TEM images of LAP-loaded lipomer suspension

Table 4: Results of LAP-loaded lipomer suspension stability study for 3 mo

Time (Months)	Storage condition	PS (nm)	PDI (%)	ZP (mV)	EE (%)	CDR (%)
0	Refrigerator temperature (4±2 °C)	88.5	0.194	-22.2	85.15	88.85
1	Refrigerator temperature (4±2 °C)	91.9	0.205	-21.4	82.01	86.21
2	Refrigerator temperature (4±2 °C)	94.50	0.231	-23.4	79.90	83.50
3	Refrigerator temperature (4±2 °C)	97.10	0.299	-22.5	76.10	82.01
0	Accelerated (40±2 °C, 75% RH)	88.5	0.194	-22.2	85.15	88.85
1	Accelerated (40±2 °C, 75% RH)	92.1	0.201	-21.1	80.12	80.12
2	Accelerated (40±2 °C, 75% RH)	99.3	0.285	-22.9	75.01	79.15
3	Accelerated (40±2 °C, 75% RH)	110.4	0.315	-20.5	72.12	76.15

### TEM of LAP-loaded lipomer suspension

The TEM micrographs of the LAP-loaded lipomer suspension fig.6 revealed predominantly spherical nanoparticles, indicating a polydisperse distribution. The particles appeared well-dispersed, without significant aggregation, confirming the successful nanoformulation. The selected area electron diffraction (SAED) pattern exhibited distinct concentric rings, suggesting the semi-crystalline nature of the lipomer.

### Accelerated stability study

Optimizing physical and chemical integrity is crucial for lipomer production, as vesicle durability affects drug retention in the polymer core and lipid layers. Over a period of three months, PS, PDI, and %EE decreased, especially under accelerated conditions (table 4), while ZP remained stable. Drug release declined slightly. The data in table 4 show a clear trend of increasing PS and PDI and decreasing %EE and %CDR over time, especially at 40 °C. This indicates physical instability (aggregation) and chemical instability (drug degradation or leakage). The formulation is "moderately stable at 4±2 °C but unstable at 40±2 °C, 75% RH".

### CONCLUSION

The study successfully developed and optimized LAP-encapsulated lipomer suspension using a QbD-based CCD approach. The optimized formulation demonstrated nanoscale PS, good surface charge, high %EE, and sustained drug release. The wide variation in particle size at the center points demonstrates that the LAP lipomer system is highly sensitive to small changes in PLA, soya lecithin, and DCM, with significant non-linear and interactive effects influencing droplet formation and particle solidification. Interactions also affect PDI, ZP, %EE, and %CDR, leading to a broad ZP range (-87 to +4 mV), where high lecithin with low PLA produces highly negative charges, and high PLA with low lecithin yields near-neutral values. Because CCD intentionally tests extreme conditions, such variability is expected and helps identify stable formulation regions. Optimizing these parameters ultimately enables more uniform particles and improved LAP drug delivery performance, which shows poor reproducibility. Comprehensive characterization confirmed the formulation's stability and compatibility. The formulation is "moderately stable at 4±2 °C but

unstable at 40±2 °C, 75% RH" over three three-month accelerated stability studies. The approach offers a simple, reproducible, and efficient method for improving LAP delivery. Overall, lipomer constitute a viable technique for increasing the effectiveness of LAP.

### FUNDING

Nil

### AUTHORS CONTRIBUTIONS

Nigar K. Mujawar: Conceptualization, methodology, analysis, data collection, writing, review, and editing. Visualization, reference search, and data interpretation. Jameel Ahmed S. Mulla: Supervision and administration of projects.

### CONFLICT OF INTERESTS

The authors express no conflicts of interest.

### REFERENCES

- Al-Mohammed HI. Development of a breathing monitor and training system and the analysis of methods of training patients to regulate their breathing when undergoing radiotherapy for lung cancer. London: City University of London; 2009.
- Guo Q, Liu L, Chen Z, Fan Y, Zhou Y, Yuan Z. Current treatments for non-small cell lung cancer. *Front Oncol.* 2022;12:945102. doi: [10.3389/fonc.2022.945102](https://doi.org/10.3389/fonc.2022.945102), PMID [36033435](https://pubmed.ncbi.nlm.nih.gov/36033435/).
- Mujawar NK, Mulla JA. Beyond boundaries: emerging trends and innovations in cancer research. In: *Horizons in cancer research*. 1<sup>st</sup> ed. Vol. 87. New York: Nova Publishers Science Publishers; 2024. p. 125-61.
- Zhang D, Pal A, Bornmann WG, Yamasaki F, Esteva FJ, Hortobagyi GN. Activity of lapatinib is independent of EGFR expression level in HER2-overexpressing breast cancer cells. *Mol Cancer Ther.* 2008;7(7):1846-50. doi: [10.1158/1535-7163.MCT-08-0168](https://doi.org/10.1158/1535-7163.MCT-08-0168), PMID [18644997](https://pubmed.ncbi.nlm.nih.gov/18644997/).
- Bartul Z, Trenor J. *Advances in Nanotechnology*. Volume 31. 1<sup>st</sup> ed. Vol. 31. New York: Nova Publishers Science Publishers. 2024. p. 171-96. doi: [10.52305/ENFL5303](https://doi.org/10.52305/ENFL5303).
- Wakaskar RR. General overview of lipid-polymer hybrid nanoparticles, dendrimers micelles liposomes, spongosomes

- and cubosomes. *J Drug Target.* 2018;26(4):311-8. doi: [10.1080/1061186X.2017.1367006](https://doi.org/10.1080/1061186X.2017.1367006), PMID 28797169.
7. Mujawar N, Mulla JA. Lipid-polymer hybrid nanoparticles in cancer therapy: a promising nanotechnology-based drug delivery system. *Int J Pharm Sci Drug Res.* 2025;17(4):371-87. doi: [10.25004/IJPSDR.2025.170408](https://doi.org/10.25004/IJPSDR.2025.170408).
  8. Shirsat AE, Chitlange SS. Application of quality by design approach to optimize process and formulation parameters of rizatriptan loaded chitosan nanoparticles. *J Adv Pharm Technol Res.* 2015;6(3):88-96. doi: [10.4103/2231-4040.157983](https://doi.org/10.4103/2231-4040.157983), PMID 26317071.
  9. Gajra B, Dalwadi C, Patel R. Formulation and optimization of itraconazole polymeric lipid hybrid nanoparticles (Lipomer) using box behnken design. *Daru.* 2015;23(1):3. doi: [10.1186/s40199-014-0087-0](https://doi.org/10.1186/s40199-014-0087-0), PMID 25604353.
  10. Dave V, Yadav RB, Kushwaha K, Yadav S, Sharma S, Agrawal U. Lipid-polymer hybrid nanoparticles: development and statistical optimization of norfloxacin for topical drug delivery system. *Bioact Mater.* 2017;2(4):269-80. doi: [10.1016/j.bioactmat.2017.07.002](https://doi.org/10.1016/j.bioactmat.2017.07.002), PMID 29744436.
  11. Nadaf SJ, Killedar SG, Kumbar VM, Bhagwat DA, Gurav SS. Pazopanib-laden lipid based nanovesicular delivery with augmented oral bioavailability and therapeutic efficacy against non-small cell lung cancer. *Int J Pharm.* 2022;628:122287. doi: [10.1016/j.ijpharm.2022.122287](https://doi.org/10.1016/j.ijpharm.2022.122287), PMID 36257467.
  12. Sopyan IY, Gozali DO, Sriwidodo IS, Guntina RK. Design-expert software (DOE): an application tool for optimization in pharmaceutical preparations formulation. *Int J App Pharm.* 2022;14(4):55-63. doi: [10.22159/ijap.2022v14i4.45144](https://doi.org/10.22159/ijap.2022v14i4.45144).
  13. Chakorkar SS, Mulla JA. Cubosome-based corticosteroidal drug delivery system for sustained ocular delivery: a pharmacokinetic investigation. *Ind J Pharm Edu Res.* 2024;58(2s):s502-14. doi: [10.5530/ijper.58.2s.52](https://doi.org/10.5530/ijper.58.2s.52).
  14. Mulla JA, Mabrouk M, Choonara YE, Kumar P, Chejara DR, du Toit LC. Development of respirable rifampicin-loaded nanoparticle composites by microemulsion-spray drying for pulmonary delivery. *J Drug Deliv Sci Technol.* 2017;41:13-9. doi: [10.1016/j.jddst.2017.06.017](https://doi.org/10.1016/j.jddst.2017.06.017).
  15. Tiwari K, Bhattacharya S. The ascension of nanosponges as a drug delivery carrier: preparation characterization and applications. *J Mater Sci Mater Med.* 2022;33(3):28. doi: [10.1007/s10856-022-06652-9](https://doi.org/10.1007/s10856-022-06652-9), PMID 35244808.
  16. Sharma S, Rasool HI, Palanisamy V, Mathisen C, Schmidt M, Wong DT. Structural-mechanical characterization of nanoparticle exosomes in human saliva using correlative AFM, FESEM, and force spectroscopy. *ACS Nano.* 2010;4(4):1921-6. doi: [10.1021/nn901824n](https://doi.org/10.1021/nn901824n), PMID 20218655.
  17. Koyama A, Miyauchi S, Morooka K, Hojo H, Einaga H, Murakami Y. Analysis of TEM images of metallic nanoparticles using convolutional neural networks and transfer learning. *J Magn Mater.* 2021;538:168225. doi: [10.1016/j.jmmm.2021.168225](https://doi.org/10.1016/j.jmmm.2021.168225).
  18. Nadaf SJ, Killedar SG. Curcumin nanocochleates: use of design of experiments solid state characterization *in vitro* apoptosis and cytotoxicity against breast cancer MCF-7 cells. *J Drug Deliv Sci Technol.* 2018;47:337-50. doi: [10.1016/j.jddst.2018.06.026](https://doi.org/10.1016/j.jddst.2018.06.026).
  19. Verma D, Thakur PS, Padhi S, Khuroo T, Talegaonkar S, Iqbal Z. Design expert assisted nanoformulation design for co-delivery of topotecan and thymoquinone: optimization *in vitro* characterization and stability assessment. *J Mol Liq.* 2017;242:382-94. doi: [10.1016/j.molliq.2017.07.002](https://doi.org/10.1016/j.molliq.2017.07.002).
  20. Birla D, Khandale N, Bashir B, Shahbaz Alam M, Vishwas S, Gupta G. Application of quality by design in optimization of nanoformulations: principle perspectives and practices. *Drug Deliv Transl Res.* 2025;15(3):798-830. doi: [10.1007/s13346-024-01681-z](https://doi.org/10.1007/s13346-024-01681-z), PMID 39126576.
  21. Yang F, Cabe M, Nowak HA, Langert KA. Chitosan/poly(lactic-co-glycolic)acid nanoparticle formulations with finely-tuned size distributions for enhanced mucoadhesion. *Pharmaceutics.* 2022;14(1):95. doi: [10.3390/pharmaceutics14010095](https://doi.org/10.3390/pharmaceutics14010095), PMID 35056991.
  22. Chettupalli AK, Ajmera S, Amarachinta PR, Manda RM, Jadi RK. Quality by design approach for preparation characterization and statistical optimization of naproxen sodium-loaded ethosomes via transdermal route. *Curr Bioact Compd.* 2023;19(10):79-98. doi: [10.2174/1573407219666230606142116](https://doi.org/10.2174/1573407219666230606142116).
  23. Zatorska M, Lazarski G, Maziarz U, Wilkosz N, Honda T, Yusa SI. Drug-loading capacity of polylactide-based micro and nanoparticles experimental and molecular modeling study. *Int J Pharm.* 2020;591:120031. doi: [10.1016/j.ijpharm.2020.120031](https://doi.org/10.1016/j.ijpharm.2020.120031), PMID 33130219.
  24. Chang CE, Hsieh CM, Huang SC, Su CY, Sheu MT, Ho HO. Lecithin-stabilized polymeric micelles (LsbPMS) for delivering quercetin: pharmacokinetic studies and therapeutic effects of quercetin alone and in combination with doxorubicin. *Sci Rep.* 2018;8(1):17640. doi: [10.1038/s41598-018-36162-0](https://doi.org/10.1038/s41598-018-36162-0), PMID 30518853.
  25. Verma D, Thakur PS, Padhi S, Khuroo T, Talegaonkar S, Iqbal Z. Design expert assisted nanoformulation design for co-delivery of topotecan and thymoquinone: optimization *in vitro* characterization and stability assessment. *J Mol Liq.* 2017;242:382-94. doi: [10.1016/j.molliq.2017.07.002](https://doi.org/10.1016/j.molliq.2017.07.002).
  26. Alam P, Shakeel F, Foudah AI, Alshehri S, Salfi R, Alqarni MH. Central composite design (CCD) for the optimisation of ethosomal gel formulation of *Punica granatum* extract: *in vitro* and *in vivo* evaluations. *Gels.* 2022;8(8):511. doi: [10.3390/gels8080511](https://doi.org/10.3390/gels8080511), PMID 36005111.
  27. Barman A, Das M, Pathak VK. Optimization of magnetic field-assisted finishing process during nanofinishing of titanium alloy (grade-5) implant using soft computing approaches. *Int J Modell Simul.* 2022;42(6):920-35. doi: [10.1080/02286203.2021.2001720](https://doi.org/10.1080/02286203.2021.2001720).
  28. Myers RH, Montgomery DC, Anderson-Cook CM. Response surface methodology: process and product optimization using designed experiments. Hoboken, NJ: John Wiley & Sons; 2016.